Acta Cryst E CRYSTALLOGRAPHIC COMMUNICATIONS

ISSN 2056-9890

Crystal structures of spinel-type Na_2MoO_4 and Na_2WO_4 revisited using neutron powder diffraction

A. Dominic Fortes

ISIS Facility, Rutherford Appleton Laboratory, Harwell Science and Innovation Campus, Didcot, Oxfordshire OX11 0QX, England, Department of Earth Sciences, University College London, Gower Street, London WC1E 6BT, England, and Department of Earth and Planetary Sciences, Birkbeck, University of London, Malet Street, London WC1E 7HX, England. *Correspondence e-mail: andrew.fortes@ucl.ac.uk

Received 24 April 2015
Accepted 5 May 2015

Edited by M. Weil, Vienna University of Technology, Austria

Keywords: neutron powder diffraction; sodium molybdate; sodium tungstate

CCDC references: 1063434; 1063433
Supporting information: this article has supporting information at journals.iucr.org/e

Time-of-flight neutron powder diffraction data have been collected from Na_2MoO_4 and Na_2WO_4 to a resolution of $\sin(\theta)/\lambda = 1.25$ Å^{-1}, which is substantially better than the previous analyses using Mo $K\alpha$ X-rays, providing roughly triple the number of measured reflections with respect to the previous studies [Okada *et al.* (1974). *Acta Cryst.* B**30**, 1872–1873; Bramnik & Ehrenberg (2004). *Z. Anorg. Allg. Chem.* **630**, 1336–1341]. The unit-cell parameters are in excellent agreement with literature data [Swanson *et al.* (1962). NBS Monograph No. 25, sect. 1, pp. 46–47] and the structural parameters for the molybdate agree very well with those of Bramnik & Ehrenberg (2004). However, the tungstate structure refinement of Okada *et al.* (1974) stands apart as being conspicuously inaccurate, giving significantly longer W—O distances, 1.819 (8) Å, and shorter Na—O distances, 2.378 (8) Å, than are reported here or in other simple tungstates. As such, this work represents an order-of-magnitude improvement in precision for sodium molybdate and an equally substantial improvement in both accuracy *and* precision for sodium tungstate. Both compounds adopt the spinel structure type. The Na^+ ions have site symmetry $.\bar{3}m$ and are in octahedral coordination while the transition metal atoms have site symmetry $\bar{4}3m$ and are in tetrahedral coordination.

1. Chemical context

Both Na_2MoO_4 and Na_2WO_4 have rich phase diagrams in pressure and temperature space (Pistorius, 1966). The stable form at room temperature is the β-Ag_2MoO_4 cubic spinel structure type, space group $Fd\bar{3}m$, which has been known for almost a century (Wyckoff, 1922). Among the alkali metal sulfates, chromates, molybdates and tungstates, only Na_2MoO_4 and Na_2WO_4 adopt the normal spinel structure at ambient pressure. Li_2MoO_4 forms a cubic spinel structure at high pressure (Liebertz & Rooymans, 1967). Li_2WO_4 forms a 'spinel-like' phase at high pressure (Pistorius, 1975; Horiuchi *et al.*, 1979). Cubic sodium molybdate and sodium tungstate have been examined intermittently over subsequent decades using a variety of crystallographic techniques (Lindqvist, 1950; Becka & Poljak, 1958; Swanson *et al.*, 1957, 1962; Singh Mudher *et al.*, 2005) and vibrational spectroscopic methods (Busey & Keller, 1964; Preudhomme & Tarte, 1972; Breitinger *et al.*, 1981; Luz Lima *et al.*, 2010, 2011), or by nuclear magnetic resonance and quadrupole coupling (Lynch & Segel, 1972). However, the extant structural information on both phases is derived from X-ray diffraction data of low to modest precision. The first published structure refinement of Na_2MoO_4 was only reported recently (Bramnik & Ehrenberg, 2004) from X-ray powder diffraction data measured to $\sin(\theta)/\lambda = 0.71$ Å^{-1}; the last structure refinement of Na_2WO_4 was

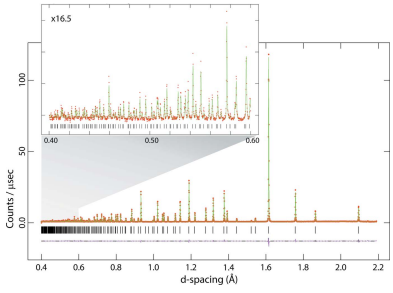

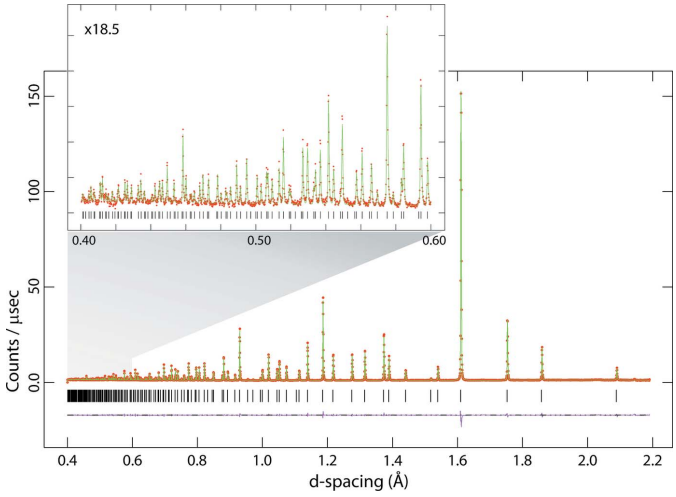

Figure 1
Neutron powder diffraction data for Na_2MoO_4; red points are the observations, the green line is the calculated profile and the pink line beneath the diffraction pattern represents Obs − Calc. Vertical black tick marks report the expected positions of the Bragg peaks. The inset shows the data measured at very short flight times (*i.e.*, small *d*-spacing).

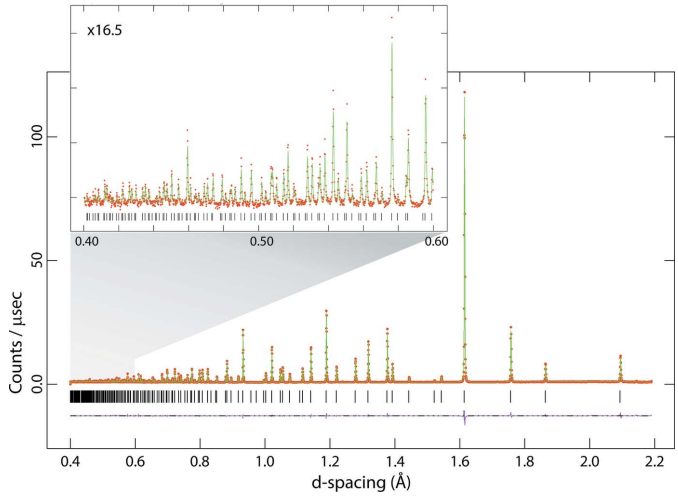

Figure 2
Neutron powder diffraction data for Na_2WO_4; red points are the observations, the green line is the calculated profile and the pink line beneath the diffraction pattern represents Obs − Calc. Vertical black tick marks report the expected positions of the Bragg peaks. The inset shows the data measured at very short flight times (*i.e.*, small *d*-spacing).

reported by Okada *et al.* (1974) from X-ray single-crystal diffraction data to sin $(\theta)/\lambda = 0.81$ Å^{-1}. Both compounds are highly soluble in water, crystallizing at room temperature as orthorhombic dihydrates (space group *Pbca*, Atovmyan & D'yachenko, 1969; Farrugia, 2007). Below 283.5 K for the molybdate and 279.2 K for the tungstate, crystals grow with ten water molecules per formula unit (Funk, 1900; Cadbury, 1955; Zhilova *et al.*, 2008). The high solubility in water and propensity towards forming hydrogen-bonded hydrates (unlike the heavier alkali metal molybdates and tungstates) suggests that both compounds would be excellent candidates for formation of hydrogen-bonded complexes with water soluble organics, such as amino acids, producing metal–organic crystals with potentially useful optical properties (*cf.*, glycine lithium molybdate; Fleck *et al.*, 2006).

In the course of preparing deuterated specimens of the dihydrated and decahydrated forms of Na_2MoO_4 and Na_2WO_4 for neutron diffraction analysis, the anhydrous phases were synthesised and an opportunity arose to acquire neutron powder diffraction data. The advantage of using a neutron radiation probe is that the scattering lengths of the atoms concerned are fairly similar, coherent scattering lengths being 6.715 fm for Mo, 4.86 fm for W, 3.63 fm for Na and 5.803 fm for O (Sears, 2006). Secondly, with the time-of-flight method, particularly with a very long primary flight path and high-angle backscattering detectors, one can acquire unparalleled resolution at very short flight times (*i.e.*, small *d*-spacings), ensuring an order of magnitude improvement in parameter precision over the previous studies. In this work, usable data were obtained at a resolution of sin $(\theta)/\lambda = 1.25$ Å^{-1}, roughly tripling the number of measured reflections with respect to Okada *et al.* (1974) and Bramnik & Ehrenberg (2004). This work provides the most accurate and precise foundation on which to build future discussion of the hydrated forms of Na_2MoO_4 and Na_2WO_4. Neutron powder diffraction data for Na_2MoO_4 and Na_2WO_4 are given in Figs. 1 and 2.

2. Structural commentary

The structure of both compounds is the normal spinel type with Na^+ ions on the 16*c* sites in octahedral coordination and Mo^{6+}/W^{6+} ions on 8*b* sites in tetrahedral coordination. The coordinating oxygen atoms occupy the 32*e* general positions, their location being defined by a single variable parameter *u*. For ideal cubic close packing, the *u* coordinate adopts a value of 0.25 although for various spinels is found in the range 0.24 to 0.275. In Na_2MoO_4 the *u* parameter has a value of 0.262710 (15) and in Na_2WO_4 it has a value of 0.262246 (15). The practical consequence of this compared with the 'ideal' value of $u = 0.25$ is that the shared edges of the NaO_6 octahedra are shorter than the unshared edges (Fig. 3*b*). In the

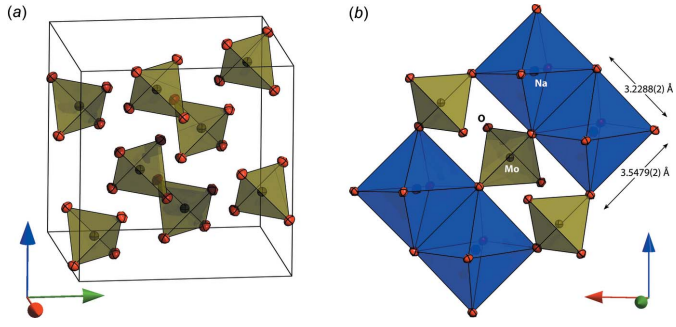

Figure 3
(*a*) Arrangement of molybdate ions in the unit cell of Na_2MoO_4; anisotropic displacement ellipsoids are drawn at the 75% probability level. (*b*) Connectivity of the NaO_6 octahedra, with shorter shared edges and longer unshared edges, to the MoO_4 tetrahedra in Na_2MoO_4; as in (*a*), the ellipsoids are drawn at the 75% probability level.

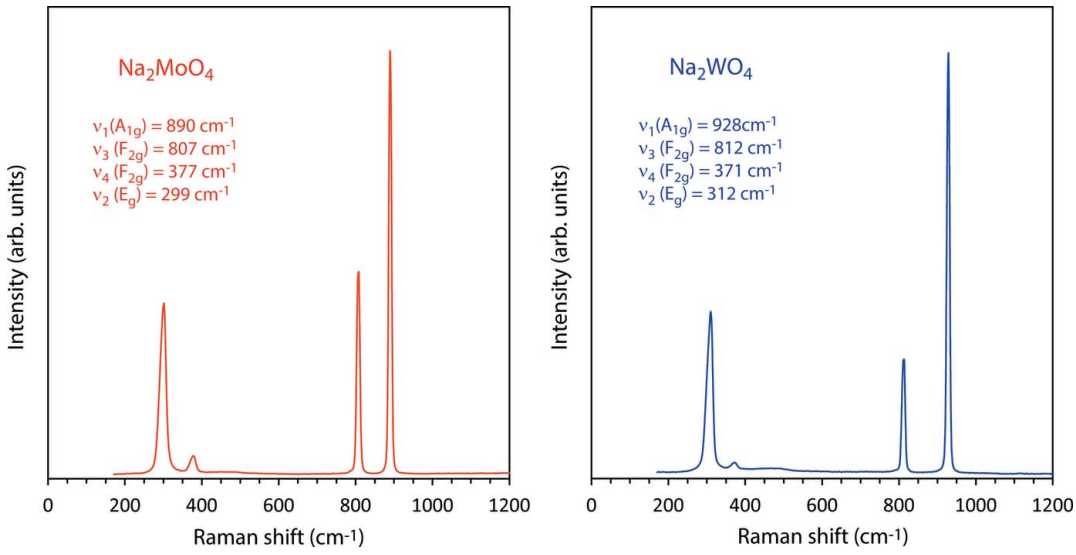

Figure 4
Raman spectra of Na_2MoO_4 (left) and Na_2WO_4 (right) in the range 0–1200 cm^{-1} (the full range of data to 4000 cm^{-1} is given in the electronic supplement). Band positions and vibrational assignments are indicated. For the tungstate these agree very well with literature values (*e.g.*, Busey & Keller, 1964) whereas for the molybdate, these data show a systematic shift to lower frequencies by 3–4 wavenumbers with respect to published values (Luz Lima *et al.*, 2010, 2011).

molybdate, these lengths are 3.2288 (2) and 3.5479 (2) Å, the ratio being 1.0988 (1); in the tungstate, the lengths of the two inequivalent octahedral edges are 3.2356 (2) Å and 3.5441 (2) Å, their ratio being 1.0953 (1). The MoO_4^{2-} and WO_4^{2-} tetrahedra have perfect T_d symmetry with Mo—O and W—O bond lengths of 1.7716 (3) and 1.7830 (2) Å, respectively. The unit-cell parameters for both compounds are in excellent agreement with those of Swanson *et al.* (1962) and the structural parameters for the molybdate agree very well with those of Bramnik & Ehrenberg (2004). However, the Na_2WO_4 structure refinement of Okada *et al.* (1974) stands apart as being conspicuously inaccurate, giving significantly longer W—O distances, 1.819 (8) Å, and shorter Na—O distances, 2.378 (8) Å, than are reported here or in many other simple tungstates. Indeed the ionic radii of four-coordinated Mo^{6+} and W^{6+} obtained from analysis of a large range of crystal structures are nearly identical, being 0.41 and 0.42 Å, respectively (Shannon, 1976). The values reported here agree very well with the majority of Mo—O and W—O bond lengths in isolated MoO_4^{2-} and WO_4^{2-} tetrahedral oxyanions from a range of alkali metal and alkaline earth compounds tabulated in the literature (*e.g.*, Zachariasen & Plettinger, 1961; Gatehouse & Leverett, 1969; Koster *et al.*, 1969; Gürmen *et al.*, 1971; Wandahl & Christensen, 1987; Farrugia, 2007; van den Berg & Juffermans, 1982). As such, this work represents an improvement in accuracy for sodium molybdate and an improvement in both accuracy and precision for sodium tungstate.

3. Synthesis and crystallization

$Na_2MoO_4{\cdot}2H_2O$ (Sigma Aldrich M1003, > 99.5%) and $Na_2WO_4{\cdot}2H_2O$ (Sigma Aldrich 14304, > 99.0%) were heated to 673 K in ceramic crucibles for 24 hr. Loss of water was confirmed by Raman spectroscopy; X-ray powder diffraction confirmed the phase identity and purity of the two anhydrous products, Na_2MoO_4 and Na_2WO_4.

Raman spectra were acquired using a B&WTek *i*-Raman plus portable spectrometer; this device uses a 532 nm laser (37 mW power at the fiber-optic probe tip) to stimulate Raman scattering, which is measured in the range 170–4000 cm^{-1} with a spectral resolution of 3 cm^{-1}. Data were collected in a series of 20 x 9 sec integrations for Na_2MoO_4 and 20 x 7 sec integrations for Na_2WO_4; after summation, the background was removed and peaks fitted using Pseudo-Voigt functions in *OriginPro* (OriginLab, Northampton, MA) (Fig. 4). These data are provided as an electronic supplement in the form of an ASCII file.

4. Refinement

Crystal data, data collection and structure refinement details are summarized in Table 1. For the neutron scattering experiments, each specimen was loaded into a vanadium tube of 11 mm internal diameter to a depth of approximately 25 mm. The exact sample volume and mass were measured in order to determine the number density for correction of the specimen self-shielding. The samples were mounted on the HRPD beamline (Ibberson, 2009) at the ISIS neutron spallation source and data were collected in the 10–110 ms time-of-flight window for 2.5 h (Na_2MoO_4) and 3.5 h (Na_2WO_4). Data were corrected for self-shielding, focussed to a common scattering angle and normalized to the incident spectrum by reference to a V:Nb null-scattering standard before being output in a format suitable for Rietveld refinement with *GSAS/Expgui* (Larsen & Von Dreele, 2000: Toby, 2001).

Table 1
Experimental details.

	Na_2MoO_4	Na_2WO_4
Crystal data		
Chemical formula	Na_2MoO_4	Na_2WO_4
M_r	205.92	293.83
Crystal system, space group	Cubic, $Fd\bar{3}m$	Cubic, $Fd\bar{3}m$
Temperature (K)	298	298
a (Å)	9.10888 (3)	9.12974 (4)
V (Å^3)	755.78 (1)	760.98 (1)
Z	8	8
Radiation type	Neutron	Neutron
μ (mm^{-1})	0.014 + 0.0018 * λ	0.014 + 0.0097 * λ
Specimen shape, size (mm)	Cylinder, 25 × 11	Cylinder, 27 × 11
Data collection		
Diffractometer	HRPD, high-resolution neutron powder	HRPD, high-resolution neutron powder
Specimen mounting	Vanadium tube	Vanadium tube
Data collection mode	Transmission	Transmission
Scan method	Time of flight	Time of flight
Absorption correction	Analytical	Analytical
2θ values (°)	$2\theta_{fixed}$ = 168.329	$2\theta_{fixed}$ = 168.329
Distance from source to specimen (mm)	95000	95000
Distance from specimen to detector (mm)	965	965
Refinement		
R factors and goodness of fit	R_p = 0.037, R_{wp} = 0.043, R_{exp} = 0.022, $R(F^2)$ = 0.06364, χ^2 = 3.842	R_p = 0.037, R_{wp} = 0.044, R_{exp} = 0.024, $R(F^2)$ = 0.06245, χ^2 = 3.423
No. of data points	7716	7716
No. of parameters	24	24

Computer programs: *HRPD control software*, *GSAS/Expgui* (Larsen & Von Dreele, 2000; Toby, 2001), *MANTID* (Arnold *et al.*, 2014; Mantid, 2013), *DIAMOND* (Putz & Brandenburg, 2006) and *publCIF* (Westrip, 2010).

Acknowledgements

The author thanks the STFC ISIS facility for beam-time access and acknowledges financial support from the STFC, grant No. ST/K000934/1.

References

Arnold, O., & 27 co-authors (2014). *Nucl. Instrum. Methods Phys. Res. A*, **764**, 156–166.
Atovmyan, L. O. & D'yachenko, O. A. (1969). *J. Struct. Chem.* **10**, 416–418.
Becka, L. N. & Poljak, R. J. (1958). *Anales Asoc. Quim. Arg.* **46**, 204–209.
Berg, A. J. van den & Juffermans, C. A. H. (1982). *J. Appl. Cryst.* **15**, 114–116.
Bramnik, K. G. & Ehrenberg, H. (2004). *Z. Anorg. Allg. Chem.* **630**, 1336–1341.
Breitinger, D. K., Emmert, L. & Kress, W. (1981). *Ber. Bunsenges. Phys. Chem.* **85**, 504–505.
Busey, R. H. & Keller, O. L. Jr (1964). *J. Chem. Phys.* **41**, 215–225.
Cadbury, W. E. Jr (1955). *J. Phys. Chem.* **59**, 257–260.
Farrugia, L. J. (2007). *Acta Cryst.* E**63**, i142.
Fleck, M., Schwendtner, K. & Hensler, A. (2006). *Acta Cryst.* C**62**, m122–m125.
Funk, R. (1900). *Ber. Dtsch. Chem. Ges.* **33**, 3696–3703.
Gatehouse, B. M. & Leverett, P. (1969). *J. Chem. Soc. A*, pp. 849.
Gürmen, E. (1971). *J. Chem. Phys.* **55**, 1093–1097.
Horiuchi, H., Morimoto, N. & Yamaoka, S. (1979). *J. Solid State Chem.* **30**, 129–135.
Ibberson, R. M. (2009). *Nucl. Instrum. Methods Phys. Res. A*, **600**, 47–49.
Koster, A. S., Kools, F. X. N. M. & Rieck, G. D. (1969). *Acta Cryst.* B**25**, 1704–1708.
Larsen, A. C. & Von Dreele, R. B. (2000). *General Structure Analysis System (GSAS)*. Los Alamos National Laboratory Report LAUR 86-748, Los Alamos, New Mexico, USA. http://www.ncnr.NIST.gov/Xtal/software/GSAS.html.
Liebertz, J. & Rooymans, C. J. M. (1967). *Solid State Commun.* **5**, 405–409.
Lindqvist, I. (1950). *Acta Chem. Scand.* **4**, 1066–1074.
Luz Lima, C., Saraiva, G. D., Freire, P. T. C., Maczka, M., Paraguassu, W., de Sousa, F. F. & Mendes Filho, J. (2011). *J. Raman Spectrosc.* **42**, 799–802.
Luz Lima, C., Saraiva, G. D., Souza Filho, A. G., Paraguassu, W., Freire, P. T. C. & Mendes Filho, J. (2010). *J. Raman Spectrosc.* **41**, 576–581.
Lynch, G. F. & Segel, S. L. (1972). *Can. J. Phys.* **50**, 567–572.
Mantid (2013). *Manipulation and Analysis Toolkit for Instrument Data; Mantid Project.* http://dx.doi.org/10.5286/SOFTWARE/MANTID.
Okada, K., Morikawa, H., Marumo, F. & Iwai, S. (1974). *Acta Cryst.* B**30**, 1872–1873.
Pistorius, C. W. F. T. (1966). *J. Chem. Phys.* **44**, 4532–4537.
Pistorius, C. W. F. T. (1975). *J. Solid State Chem.* **13**, 325–329.
Preudhomme, J. & Tarte, P. (1972). *Spectrochim. Acta Part A*, **28**, 69–79.
Putz, H. & Brandenburg, K. (2006). *DIAMOND*. Crystal Impact GbR, Bonn, Germany. http://www.crystalimpact.com/diamond.
Sears, V. F. (2006). *Neutron News*, **3**, 26–37.
Shannon, R. D. (1976). *Acta Cryst.* A**32**, 751–767.
Singh Mudher, K. D., Keskar, M., Krishnan, K. & Venugopal, V. (2005). *J. Alloys Compd.* **396**, 275–279.
Swanson, H. E., Gilfrich, N. T. & Cook, M. I. (1957). Natl. Bur. Stand. (US) Circ. 539, Vol. 7, p. 45.
Swanson, H. E., Morris, M. C., Stinchfield, R. P. & Evans, E. H. (1962). NBS Monograph No. 25, sect. 1, pp. 46–47.
Toby, B. H. (2001). *J. Appl. Cryst.* **34**, 210–213.

Wandahl, G. & Christensen, A. N. (1987). *Acta Chem. Scand. Ser. A*, **41**, 358–360.
Westrip, S. P. (2010). *J. Appl. Cryst.* **43**, 920–925.
Wyckoff, R. W. G. (1922). *J. Am. Chem. Soc.* **44**, 1994–1998.
Zachariasen, W. H. & Plettinger, H. A. (1961). *Acta Cryst.* **14**, 229–230.
Zhilova, S. B., Karov, Z. G. & El'mesova, R. M. (2008). *Russ. J. Inorg. Chem.* **53**, 628–635.

supporting information

Acta Cryst. (2015). E**71**, 592-596 [doi:10.1107/S2056989015008774]

Crystal structures of spinel-type Na_2MoO_4 and Na_2WO_4 revisited using neutron powder diffraction

A. Dominic Fortes

Computing details

For both compounds, data collection: *HRPD control software*; cell refinement: *GSAS/Expgui* (Larsen & Von Dreele, 2000; Toby, 2001); data reduction: *MANTID* (Arnold *et al.*, 2014; Mantid, 2013); program(s) used to solve structure: coordinates taken from a previous refinement. Program(s) used to refine structure: *GSAS/Expgui* (Larsen & Von Dreele, 2000, Toby, 2001) for Na2MoO4; *GSAS/Expgui* (Larsen & Von Dreele, 2000; Toby, 2001) for Na2WO4. For both compounds, molecular graphics: *DIAMOND* (Putz & Brandenburg, 2006); software used to prepare material for publication: *publCIF* (Westrip, 2010).

(Na2MoO4) Disodium molybdenum(VI) oxide

Crystal data

Na_2MoO_4
M_r = 205.92
Cubic, $Fd\bar{3}m$
Hall symbol: -F 4vw 2vw 3
a = 9.10888 (3) Å
V = 755.78 (1) Å^3
Z = 8
D_x = 3.619 Mg m^{-3}
Melting point: 961 K
Neutron radiation
μ = 0.01+ 0.0018 * λ mm^{-1}
T = 298 K
white
cylinder, 25 × 11 mm
Specimen preparation: Prepared at 673 K and 100 kPa

Data collection

HRPD, High resolution neutron powder diffractometer
Radiation source: ISIS Facility, Neutron spallation source
Specimen mounting: vanadium tube
Data collection mode: transmission
Scan method: time of flight
Absorption correction: analytical
Data were corrected for self shielding using σ_{scatt} = 29.198 barns and $\sigma_{ab}(\lambda)$ = 3.541 barns at 1.798 Å during the normalization procedure. The linear absorption coefficient is wavelength dependent and is calculated as: μ = 0.014 + 0.0018 * λ (mm^{-1}).
T_{min} = 1.000, T_{max} = 1.000
$2\theta_{fixed}$ = 168.329
Distance from source to specimen: 95000 mm
Distance from specimen to detector: 965 mm

Refinement

Least-squares matrix: full
$R_p = 0.037$
$R_{wp} = 0.043$
$R_{exp} = 0.022$
$R(F^2) = 0.06364$
$\chi^2 = 3.842$
7716 data points
Excluded region(s): Data at d-spacings smaller than 0.4 Å were excluded since the counting statistics became progressively poorer at very short flight times due to the lower neutron flux at the shortest wavelengths.

Profile function: TOF profile function #3 (21 terms). Profile coefficients for exp pseudovoigt convolution [Von Dreele, 1990 (unpublished)] (α) = 0.1919, (β_0) = 0.025953, (β_1) = 0.005213, (σ_0) = 0, (σ_1) = 196.3, (σ_2) = 23.5, (γ_0) = 0, (γ_1) = 14.91, (γ_2) = 0, (γ_{2s}) = 0, (γ_{1e}) = 0, (γ_{2e}) = 0, (ε_i) = 0, (ε_a) = 0, (ε_A) = 0, (γ_{11}) = 0, (γ_{22}) = 0, (γ_{33}) = 0, (γ_{12}) = 0, (γ_{13}) = 0, (γ_{23}) = 0. Peak tails ignored where intensity <0.0005x peak. Aniso. broadening axis 0.0 0.0 1.0
24 parameters
0 restraints
0 constraints
$(\Delta/\sigma)_{max} = 0.03$
Background function: GSAS Background function #1 (10 terms). Shifted Chebyshev function of 1st kind 1: 1.18715, 2: -7.466630×10^{-3}, 3:8.117230×10^{-2}, 4: -5.411800×10^{-2}, 5: -1.714140×10^{-2}, 6: -1.882400×10^{-2}, 7: -1.930110×10^{-2}, 8: -6.255180×10^{-3}, 9: 6.598230×10^{-3}, 10: 8.478560×10^{-3}

Fractional atomic coordinates and isotropic or equivalent isotropic displacement parameters (Å²)

	x	*y*	*z*	U_{iso}*/U_{eq}
O	0.262710 (16)	0.262710 (16)	0.262710 (16)	0.01182
Mo	0.375	0.375	0.375	0.00740
Na	0.0	0.0	0.0	0.01381

Atomic displacement parameters (Å²)

	U^{11}	U^{22}	U^{33}	U^{12}	U^{13}	U^{23}
O	0.01182 (6)	0.01182 (6)	0.01182 (6)	−0.00156 (6)	−0.00156 (6)	−0.00156 (6)
Mo	0.00740 (8)	0.00740 (8)	0.00740 (8)	0.0	0.0	0.0
Na	0.01381 (11)	0.01381 (11)	0.01381 (11)	−0.00068 (12)	−0.00068 (12)	−0.00068 (12)

Geometric parameters (Å, º)

Mo—O	1.7716 (3)	Na^{iv}—O^{vii}	2.3986 (2)
Mo—O^{i}	1.7716 (3)	Na^{iv}—O^{viii}	2.3986 (2)
Mo—O^{ii}	1.7716 (3)	Na^{iv}—O^{ix}	2.3986 (2)
Mo—O^{iii}	1.7716 (3)	Na—Na^{iv}	3.2205 (1)
Na^{iv}—O	2.3986 (2)	Mo—Na^{iv}	3.7763 (1)
Na^{iv}—O^{v}	2.3986 (2)	O—O^{vi}	3.2288 (2)
Na^{iv}—O^{vi}	2.3986 (2)	O—O^{v}	3.5479 (4)
O—Mo—O^{i}	109.4712 (1)	O—Na^{iv}—O^{v}	95.393 (6)
O—Mo—O^{ii}	109.4712 (1)	O—Na^{iv}—O^{ix}	180.000 (1)
O—Mo—O^{iii}	109.4712 (1)	O—Na^{iv}—O^{viii}	84.607 (6)

O^{i}—Mo—O^{ii}	109.4712 (1)	O—Na^{iv}—O^{vii}	95.393 (6)
O^{i}—Mo—O^{iii}	109.4712 (1)	O^{v}—Na^{iv}—O^{vi}	180.000 (1)
O^{ii}—Mo—O^{iii}	109.4712 (1)	Mo—O—Na^{iv}	129.178 (5)
O—Na^{iv}—O^{vi}	84.607 (6)		

Symmetry codes: (i) $-x+3/4, y, -z+3/4$; (ii) $-x+3/4, -y+3/4, z$; (iii) $x, -y+3/4, -z+3/4$; (iv) $-x+1/4, -y+1/4, z$; (v) $x, -y+1/4, -z+1/4$; (vi) $-y+1/2, x+1/4, z-1/4$; (vii) $-x+1/4, y, -z+1/4$; (viii) $y+1/4, -x+1/2, z-1/4$; (ix) $-y+1/2, -x+1/2, -z$.

(Na2WO4) Disodium tungsten(VI) oxide

Crystal data

Na_2WO_4
$M_r = 293.83$
Cubic, $Fd\bar{3}m$
Hall symbol: -F 4vw 2vw 3
$a = 9.12974$ (4) Å
$V = 760.98$ (1) Å^3
$Z = 8$
$D_x = 5.129$ Mg m^{-3}

Melting point: 969 K
Neutron radiation
$\mu = 0.01+ 0.0097 * \lambda$ mm^{-1}
$T = 298$ K
white
cylinder, 27 × 11 mm
Specimen preparation: Prepared at 673 K and 100 kPa

Data collection

HRPD, High resolution neutron powder diffractometer
Radiation source: ISIS Facility, Neutron spallation source
Specimen mounting: vanadium tube
Data collection mode: transmission
Scan method: time of flight

Absorption correction: analytical
Data were corrected for self shielding using σ_{scatt} = 28.088 barns and $\sigma_{ab}(\lambda)$ = 19.361 barns at 1.798 Å during the normalisation procedure. The linear absorption coefficient is wavelength dependent and is calculated as: $\mu = 0.014 + 0.0097 * \lambda$ [mm^{-1}]
$T_{min} = 1.000$, $T_{max} = 1.000$
$2\theta_{fixed} = 168.329$
Distance from source to specimen: 95000 mm
Distance from specimen to detector: 965 mm

Refinement

Least-squares matrix: full
$R_p = 0.037$
$R_{wp} = 0.044$
$R_{exp} = 0.024$
$R(F^2) = 0.06245$
$\chi^2 = 3.423$
7716 data points
Excluded region(s): Data at d-spacings smaller than 0.4 Å were excluded since the counting statistics became progressively poorer at very short flight times due to the lower neutron flux at the shortest wavelengths.

Profile function: TOF profile function #3 (21 terms). Profile coefficients for exp pseudovoigt convolution [Von Dreele, 1990 (unpublished)] (α) = 0.1603, (β_0) = 0.026115, (β_1) = 0.004558, (σ_0) = 0, (σ_1) = 237.2, (σ_2) = 45.0, (γ_0) = 0, (γ_1) = 14.21, (γ_2) = 0, (γ_{2s}) = 0, (γ_{1e}) = 0, (γ_{2e}) = 0, (ε_i) = 0, (ε_a) = 0, (ε_A) = 0, (γ_{11}) = 0, (γ_{22}) = 0, (γ_{33}) = 0, (γ_{12}) = 0, (γ_{13}) = 0, (γ_{23}) = 0. Peak tails ignored where intensity <0.0005x peak. Aniso. broadening axis 0.0 0.0 1.0
24 parameters
0 restraints
0 constraints
$(\Delta/\sigma)_{max} = 0.01$
Background function: GSAS Background function # 1 (10 terms). Shifted Chebyshev function of 1st kind 1: 0.884779, 2: 4.212470x10^{-2}, 3: 4.210950x10^{-2}, 4: -4.489520x10^{-2}, 5: -2.683690x10^{-2}, 6: -1.892450x10^{-2}, 7: -2.248710x10^{-2}, 8: -2.821970x10^{-3}, 9: 6.467340x10^{-3}, 10: 6.167050x10^{-3}

Fractional atomic coordinates and isotropic or equivalent isotropic displacement parameters (Å²)

	x	*y*	*z*	U_{iso}*/U_{eq}
O	0.262246 (15)	0.262246 (15)	0.262246 (15)	0.01312
W	0.375	0.375	0.375	0.00903
Na	0.0	0.0	0.0	0.01538

Atomic displacement parameters (Å²)

	U^{11}	U^{22}	U^{33}	U^{12}	U^{13}	U^{23}
O	0.01312 (6)	0.01312 (6)	0.01312 (6)	−0.00161 (5)	−0.00161 (5)	−0.00161 (5)
W	0.00903 (11)	0.00903 (11)	0.00903 (11)	0.0	0.0	0.0
Na	0.01538 (11)	0.01538 (11)	0.01538 (11)	−0.00045 (12)	−0.00045 (12)	−0.00045 (12)

Geometric parameters (Å, º)

W—O	1.7830 (2)	Na^{iv}—O^{vii}	2.3995 (1)
W—O^{i}	1.7830 (2)	Na^{iv}—O^{viii}	2.3995 (1)
W—O^{ii}	1.7830 (2)	Na^{iv}—O^{ix}	2.3995 (1)
W—O^{iii}	1.7830 (2)	Na—Na^{iv}	3.2279 (1)
Na^{iv}—O	2.3995 (1)	W—Na^{iv}	3.7850 (1)
Na^{iv}—O^{v}	2.3995 (1)	O—O^{vi}	3.2356 (2)
Na^{iv}—O^{vi}	2.3995 (1)	O—O^{v}	3.5441 (4)
O—W—O^{i}	109.4712 (3)	O—Na^{iv}—O^{v}	95.211 (6)
O—W—O^{ii}	109.4712 (3)	O—Na^{iv}—O^{ix}	180.000 (1)
O—W—O^{iii}	109.4712 (3)	O—Na^{iv}—O^{viii}	84.789 (6)
O^{i}—W—O^{ii}	109.4712 (3)	O—Na^{iv}—O^{vii}	95.211 (6)
O^{i}—W—O^{iii}	109.4712 (3)	O^{v}—Na^{iv}—O^{vi}	180.000 (1)
O^{ii}—W—O^{iii}	109.4712 (3)	W—O—Na^{iv}	129.043 (4)
O—Na^{iv}—O^{vi}	84.789 (6)		

Symmetry codes: (i) −*x*+3/4, *y*, −*z*+3/4; (ii) −*x*+3/4, −*y*+3/4, *z*; (iii) *x*, −*y*+3/4, −*z*+3/4; (iv) −*x*+1/4, −*y*+1/4, *z*; (v) *x*, −*y*+1/4, −*z*+1/4; (vi) −*y*+1/2, *x*+1/4, *z*−1/4; (vii) −*x*+1/4, *y*, −*z*+1/4; (viii) *y*+1/4, −*x*+1/2, *z*−1/4; (ix) −*y*+1/2, −*x*+1/2, −*z*.